A stopping algorithm for mechanical systems underactuated by one control

Jason Nightingale[1], Richard Hind[2], and Bill Goodwine[1]

[1] Department of Aerospace and Mechanical Engineering, University of Notre Dame, `jnightin@nd.edu`
[2] Department of Mathematics, University of Notre Dame, `rhind@nd.edu`
[3] Department of Aerospace and Mechanical Engineering, University of Notre Dame, `jgoodwin@nd.edu`

Abstract: Analysis and control of underactuated mechanical systems in the nonzero velocity setting remains a challenging problem. In this paper, we demonstrate the utility of a recently developed alternative representation of the equations of motion for this large class of nonlinear control systems. The alternative representation gives rise to an intrinisic symmetric form. The generalized eigenvalues and eigenvectors associated with the symmetric form are used to determine control inputs that will drive a class of mechanical systems underactuated by one control to rest from an arbitrary initial configuration and velocity. We focus on systems whose symmetric form is indefinite for almost all configurations. Finally, we illustrate the stopping algorithm by presenting numerical simulation results for the planar rigid body, snakeboard and planar rollerblader.

1 Introduction

Mechanical control systems form a large and important subclass of nonlinear control systems. The areas of application of control theory for mechanical systems are diverse and challenging. Such areas include autonomous aerospace and marine vehicles, robotics and automation, mobile robots, and constrained systems. The formalism of affine connections and distributions on a Riemannian manifold provides an elegant framework for modeling, analysis and control. This framework has given rise to new insights into nonlinear controllability in the *zero velocity setting* motivating stabilization, tracking and motion planning algorithms [1]. For fully actuated mechanical systems, it is possible to provide a comprehensive solution to the problem of trajectory tracking [10]. In contrast, motion planning algorithm for underactuated mechanical systems is still not well understood. Due to the challenging nature of these problems, many of the existing results have been limited for example to *ad hoc* gait generation algorithms [9] [8], *ad hoc* configuration to configuration algorithms
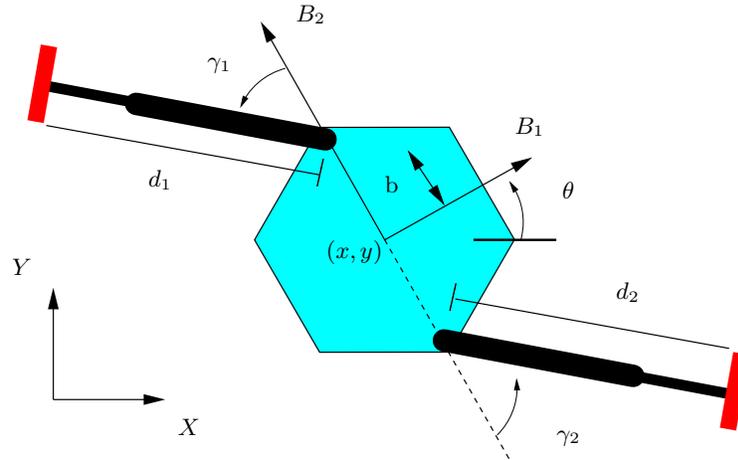
Fig. 1. A schematic of the planar rollerblader.

with zero-velocity transitions between feasible motions [3] and numerically generated optimal trajectories [4].

This paper is also closely related to several efforts that have been made to obtain conditions in the zero velocity setting from properties of a certain intrinsic vector-valued quadratic form which does not depend upon the choice of basis for the input distribution [2], [6]. It has been observed that vector-valued quadratic forms come up in a variety of areas in control theory which has motivated a new initiative to understand the geometry of these forms [7].

1.1 Motivating Example

As a concrete example, take the planar rollerblader illustrated in Figure 1. The schematic drawing illustrates the kinematics and actuator locations of the model. Note that each leg is composed of two links which are connected by a translation joint at the knee and a pin joint at the hip. The foot is a roller blade which is constrained to the plane in such a way that prohibits motion of the foot perpendicular to the blade. A single actuator capable of generating torque in both the clockwise and counterclockwise directions is placed at each pin joint. Another set of linear actuators are placed at each translation joint. The planar rollerblader has five degrees of freedom and only four actuators. This is an example of an **underactuated** control system. Whenever fewer actuators are available than degrees of freedom, various control questions arise. For instances, it is not immediately clear whether the moving rollerblader can be "stopped" using the limited control authority. If it cannot be stopped, then the set of reachable velocities does not include zero velocity. *In this, and other underactuated mechanical systems, existing geometric control theory does not provide a general test for stopping and more generally speaking, the*

set of reachable velocities from a nonzero velocity is not well understood. The modern development of geometric control of mechanical systems has been limited, for the most part, to the zero velocity setting. Yet the underlying mathematical structure is that of second-order dynamics where the state of the system is defined by a configuration and velocity. Theoretical results that are limited to zero velocity states do not provide an adequate characterization of the behavior of mechanical systems and limits the development of motion planning algorithms.

1.2 Statement of Contribution

The fundamental approach of this paper is to exploit the inherent geometric structure for the purpose of stopping an underactuated mechanical system. We use the governing equations of motion of the mechanical control system to partition or foliate the velocity-phase manifold (*e.g.* set of all configurations and velocities). This partitioning has given rise to two key theoretical results which have been the main topics of recent works [13], [14]. First, we have identified an intrinsic vector-valued symmetric bilinear form that can be associated with an underactuated mechanical control system. Second, we have provided computable tests dependent upon the definiteness of the symmetric form to determine if the system can or cannot be driven to rest.

Our theoretical results are useful for two reasons. First, such results are necessary conditions for a stopping algorithm. If zero velocity is not contained in the set of reachable states then it is impossible to specify a control law that will drive the system to rest. Second, these results are useful design tools which provide constructive strategies for actuator assignment and help to make the control scheme robust to actuator failure. The task of actuator assignment is always a balance between the sophistication of the system design and the associated complexity of the controller. For example, a system which is fully actuated requires a simple control scheme to drive it to rest. In contrast, if the system is underactuated even by just one control, a control scheme must take into account the underlying geometry or nonlinearities of the geometric model. Such a control scheme is theoretically challenging due to nonzero drift which indicates a component of the dynamics that is not directly controlled. These systems are not amendable to standard techniques in control theory. However, underactuated systems do appear in many practical applications resulting from design choices motivated by cost reductions or in some cases they are the result of a failure in fully actuated mechanical systems.

The main contribution of this paper is a stopping algorithm for mechanical systems underactuated by one control. We focus our analysis on such systems whose symmetric form is indefinite for almost all configurations. The choice of control inputs are dependent upon the generalized eigenvalues and eigenvectors associated with the symmetric form. The stopping algorithm is applied to the planar rigid body, snakeboard [9] and rollerblader [8]. For each

system, we provide a schematic drawing, the geometric model, our alternative representation and simulation results.

2 Geometric Model

2.1 Mechanical Control System

We consider a simple mechanical control system with no potential to be comprised of an n-dimensional configuration manifold M; a Riemannian metric $\mathbb{G}$ which represents the kinetic energy; m linearly independent one forms $F^1, \ldots, F^m$ on M which represents the input forces; a distribution H on M which represents the constraint; and $U = \mathbb{R}^m$ which represents the set of inputs. We do not require the set of inputs to be a subset of $\mathbb{R}^m$. This allows use to focus on the geometric properties of our system that inhibit or allow motion in the foliation as opposed to a limitation on the set of inputs. We represent the input forces as one forms and us the associated dual vector fields $Y_a = \mathbb{G}^\sharp(F^a)$, $a = 1, \ldots, m$ in our computations. Formally, we denote the control system by the tuple $\Sigma = \{M, \mathbb{G}, \mathcal{Y}, V, U\}$ where $\mathcal{Y} = \{Y_a \mid Y_a = \mathbb{G}^\sharp(F^a) \ \forall \ a\}$ is the input distribution. Note we restrict our attention to control systems where the input forces are dependent upon configuration and independent of velocity and time. DoCarmo [12] provides an excellent introduction to Riemannian geometry. A thorough description of simple mechanical control systems is provided by Bullo and Lewis [1].

It is well known that the Lagrange-d'Alembert principle can be used to generate the equations of motion for a forced simple mechanical system in coordinate invariant form. If we set the Lagrangian equal to the kinetic energy, then the equations are given by

$$\nabla_{\dot{\gamma}(t)}\dot{\gamma}(t) = u^a(t)Y_a(\gamma(t)) \tag{1}$$

where ∇ is the Levi-Civita connection corresponding to $\mathbb{G}$, u is a map from $I \subset \mathbb{R} \mapsto \mathbb{R}^M$, $\gamma : I \to M$ is a curve on M and $t \in I$. Therefore, a *controlled trajectory* for Σ is taken to be the pair (γ, u) where γ and u are defined on the same interval $I \subset \mathbb{R}$. Note the usual summation notation will be assumed over repeated indices throughout this paper.

Given a constraint distribution H of rank k, we may restrict the Levi-Civita connection ∇ to H [11]. Bullo and Zefran [5] showed that given two vector fields X and Y on M then the so-called *constrained affine connection* $\tilde{\nabla}$ is given by

$$\tilde{\nabla}_X Y = P\left(\nabla_X Y\right)$$

where P is the orthogonal projection $TM \mapsto H$. The latter approach provides a computationally efficient method and is used to generate the coordinate

expression for the constrained affine connection for the roller racer and the snakeboard.

The natural coordinates on TM are denoted by $((q^1, \ldots, q^n), (v^1, \ldots, v^n))$ where $(v^1, \ldots, v^n)$ are the coefficients of a tangent vector given the usual basis $\{\frac{\partial}{\partial q^1}, \ldots, \frac{\partial}{\partial q^n}\}$. We will denote a point in TM by v_q. We may lift the second-order differential equation defined by (1) to TM. This gives rise to the following system of first-order differential equations on TM

$$\frac{dq^k}{dt} = v^k, \tag{2}$$
$$\frac{dv^k}{dt} = -\Gamma_{ij}^k v^i v^j + u^a Y_a^k,$$

where Γ_{ij}^k is the usual Christoffel symbol and $i, j, k = 1, \ldots, n$.

A critical tool used to analyze distributions and mechanical control systems is the symmetric product. Given a pair of vector fields X, Y, their symmetric product is the vector field defined by

$$\langle X : Y \rangle = \nabla_X Y + \nabla_Y X.$$

2.2 Alternative Representation

In this section we expand upon and adapt the definition of an affine subbundle found in Hirschorn and Lewis [6]. We restrict our attention to configuration manifolds that admit a well defined global set of basis vector fields however our results generalize under appropriate conditions. *The basic geometry of our construction can be captured by assuming $H = TM$ however we can always relax this assumption by properly accounting for the orthogonal projection P.*

Recall that an input distribution $\mathcal{Y}$ on M is a subset $\mathcal{Y} \subset TM$ having the property that for each $q \in M$ there exists a family of vector fields $\{Y_1, \ldots, Y_m\}$ on M so that for each $q \in M$ we have

$$\mathcal{Y}_q \equiv \mathcal{Y} \cap T_q M = \mathrm{span}_{\mathbb{R}}\{Y_1(q), \ldots, Y_m(q)\}.$$

We refer to the vector fields $\{Y_1, \ldots, Y_m\}$ as generators for $\mathcal{Y}$. Let $\mathcal{Y}^\perp$ denote an orthonormal frame $\{Y_1^\perp, \ldots, Y_{n-m}^\perp\}$ that generates the $\mathbb{G}$-orthogonal complement of the input distribution $\mathcal{Y}$. Note that even though $\mathcal{Y}^\perp$ is canonically defined, we must choose an orthonormal basis. It is clear that $\{\mathcal{Y}_q, \mathcal{Y}_q^\perp\}$ forms a basis for $T_q M$ at each $q \in M$. Note that $\mathcal{Y} = \{Y_1, \ldots, Y_m\}$ is a set of m *linearly independent* vector fields while $\mathcal{Y}^\perp = \{Y_1^\perp, \ldots, Y_{n-m}^\perp\}$ is a set of $n - m$ *orthonormal* vector fields. This basis will be used to define an affine subbundle and construct an affine foliation of the tangent bundle.

An *affine subbundle* on M is a subset $A \subset TM$ having the property that for each $q \in M$ there exists a family of vector fields $\{Y_0, \ldots, Y_m\}$ so that for each $q \in U$ we have

$$A_q \equiv A \cap T_q M$$
$$= \{Y_0(q) = Y_1^\perp(q) + \cdots + Y_{n-m}^\perp(q)\}$$
$$+ \operatorname{span}_\mathbb{R}\{Y_1(q), \ldots, Y_m(q)\}.$$

An *affine foliation*, $\mathcal{A}$, on TM is a collection of disjoint immersed affine sub-bundles of TM whose disjoint union equals TM. Each connected affine sub-bundle A is called an *affine leaf* of the affine foliation. Now let us apply this framework to a simple mechanical control system.

Definition 1. *Let $(M, \mathbb{G}, V, \mathcal{Y}, U)$ be a simple mechanical control system with the input distribution $\mathcal{Y}$ generated by $\{Y_1, \ldots, Y_m\}$ and the corresponding $\mathbb{G}$-orthogonal distribution $\mathcal{Y}^\perp$ generated by $\{Y_1^\perp, \ldots, Y_{n-m}^\perp\}$. An **input foliation** $\mathcal{A}_\mathcal{Y}$ is an affine foliation whose affine leaves are affine subbundles given by*

$$A_s(q) = \{v_q \in TM \mid \langle\langle Y^\perp, v_q\rangle\rangle = s, s \in \mathbb{R}^{n-m}\}.$$

Remark 1. The input foliation is parametrized by $s \in \mathbb{R}^{n-m}$. Note that when $s = 0$, $A_0 = \mathcal{Y}$ and $A_0(q) = \mathcal{Y}_q$ where $\mathcal{Y}$ is an immersed submanifold of TM and $\mathcal{Y}_q$ is a linear subspace of $T_q M$. Thus, the input distribution $\mathcal{Y}$ is a single leaf of the affine foliation.

Given a basis of vector fields $\{X_1, \ldots, X_n\}$ on M, we define the *generalized Christoffel symbols* of ∇ to be

$$\nabla_{X_i} X_j = \hat{\Gamma}_{ij}^k X_k.$$

Note that when $X_i = \frac{\partial}{\partial q^i}$ we recover the usual Christoffel symbols of ∇. We introduce the *symmetrization* of the generalized Christoffel symbols.

Definition 2. *We define the **generalized symmetric Christoffel symbols** for ∇ with respect to the basis of vector fields $\{X_1, \ldots, X_n\}$ on M as the n^3 functions $\tilde{\Gamma}_{ij}^k : M \to \mathbb{R}$ defined by*

$$\tilde{\Gamma}_{ij}^k X_k = \frac{1}{2}\left(\hat{\Gamma}_{ij}^k + \hat{\Gamma}_{ji}^k\right) X_k$$
$$= \frac{1}{2}\langle X_i : X_j\rangle.$$

We may define the velocity vector $\dot{\gamma}(t) = \dot{\gamma}^i(t)\frac{\partial}{\partial q^i}$ of the curve $\gamma(t)$ in terms of the family of vector fields $\{\mathcal{Y}, \mathcal{Y}^\perp\}$. The new expression for $\dot{\gamma}(t)$ is in the form

$$\dot{\gamma}(t) = w^a(t)Y_a(\gamma(t)) + s^b(t)Y_b^\perp(\gamma(t)) \tag{3}$$

where $s^b(t) = \langle\langle\dot{\gamma}(t), Y_b^\perp\rangle\rangle_{\gamma(t)}$. We now provide a local expression for a measure of a simple mechanical control system's ability to move among the leaves of the input foliation $\mathcal{A}_\mathcal{Y}$.

Lemma 1. *Let $(M, \mathbb{G}, V, \mathcal{Y}, U)$ be a simple mechanical control system with an input foliation $\mathcal{A}_\mathcal{Y}$ defined above. The following holds along the curve $\gamma(t)$ satisfying (1):*

$$\frac{d}{dt}s^b(t) = -\frac{1}{2}w^a(t)w^p(t)\langle\langle\langle Y_a : Y_p\rangle, Y_b^\perp\rangle\rangle \qquad (4)$$

$$-\frac{1}{2}w^a(t)s^r(t)\langle\langle\langle Y_a : Y_r^\perp\rangle, Y_b^\perp\rangle\rangle$$

$$-\frac{1}{2}s^r(t)w^p(t)\langle\langle\langle Y_r^\perp : Y_p\rangle, Y_b^\perp\rangle\rangle$$

$$-\frac{1}{2}s^r(t)s^k(t)\langle\langle\langle Y_r^\perp : Y_k^\perp\rangle, Y_b^\perp\rangle\rangle$$

where $a, p \in \{1, \ldots, m\}$, $b, k, r \in \{1, \ldots, n - m\}$.

Proof. Recall from the definition of an input foliation that

$$s^b(t) = \langle\langle Y_b^\perp, \dot{\gamma}(t)\rangle\rangle. \qquad (5)$$

We could proceed by substituting (3) into (5) and differentiating taking advantage of the compatibility associated with the Levi-Civita connection. Alternatively, we use the notion of a generalized symmetric Christoffel symbol. It follows from the construction of $\mathcal{Y}^\perp$ that the bth component of $\tilde{\Gamma}_{ij}^b$ along the the orthonormal vector field $Y_b^\perp$ can be expressed as a projection using $\mathbb{G}$.

We observe that (5) is quadratic in the parameter $w(t)$. Now we relate an intrinsic vector-valued symmetric bilinear form to the measure derived in Lemma 1.

Definition 3. *Let $(M, \mathbb{G}, V, \mathcal{Y}, U)$ be a simple mechanical control system with the input distribution $\mathcal{Y}$ generated by $\{Y_1, \ldots, Y_m\}$ and the corresponding $\mathbb{G}$-orthogonal distribution $\mathcal{Y}^\perp$ generated by $\{Y_{m+1}^\perp, \ldots, Y_n^\perp\}$. We define the **intrinsic vector-valued symmetric bilinear form** to be $B : \mathcal{Y}_q \times \mathcal{Y}_q \to \mathrm{d}_q^\perp$ given in coordinates by*

$$B_{ap}^b w^a w^p = \frac{1}{2}\langle\langle\langle Y_a : Y_p\rangle, Y_b^\perp\rangle\rangle w^a w^p,$$

where $a, p \in \{1, \ldots, m\}, b \in \{1, \ldots, n - m\}$.

Remark 2. If Σ is underactuated by one control then $b = 1$ and B is a real-valued symmetric bilinear form.

The intrinsic vector-valued symmetric bilinear form defined above is an important measure of how the velocity components w parallel to the input forces influence the velocity components s orthogonal to the input forces. The remainder of the paper will detail the properties of B that form the foundation for the stopping algorithm.

3 Stopping Algorithm

The stopping algorithm consists of three simple stages. The first stage of the algorithm is driving the w-velocities towards the appropriate eigenvector. Recall that the symmetric form measures the influence the w-velocities have on the s-velocity. If we wish to decrease the s-velocity then we drive the w-velocities toward the eigenvector associated with the most negative eigenvalue of the symmetric form. In contrast, if we desire to increase the s-velocity then we drive the w-velocities toward the eigenvector associated with the most positive eigenvalue of the symmetric form. For this paper, we assume that the symmetric form is indefinite for almost all configurations. This guarantees the existence of both positive and negative eigenvalues.

The second stage of the algorithm consists of driving w-velocities along the appropriate eigenvector. The third stage of the algorithm consists of driving the w-velocities to zero. This is achieved by choosing a control input directly opposing the current w-velocities. The stopping algorithm cycles through each stage until the magnitude of each velocity component drops below a specified bound. The cycling can be observed in the simulation results for three different mechanical systems underactuated by one control found in Section 4.

4 Examples

4.1 Planar Rigid Body

In this section we review the geometric model of the planar rigid body (Fig. 2).

The configuration manifold for the system is the Lie group $SE(2)$ and the potential function is assumed to be identically zero. Let us use coordinates (x, y, θ) for the planar robot where (x, y) describes the position of the center of mass and θ describes the orientation of the body frame $\{b_1, b_2\}$ with respect to the inertial frame $\{e_1, e_2\}$. In these coordinates, the Riemannian metric is given by

$$\mathbb{G} = m dx \otimes dx + m dy \otimes dy + J d\theta \otimes d\theta,$$

where m is the mass of the body and J is the moment of inertia about the center of mass. The inputs for this system consist of two independent forces applied to an arbitrary point. We assume that the point of application of the force is a distance $h > 0$ from the center of mass along the b_1 body-axis. Physically, the input force can be thought of as a variable-direction thruster on the body which can be resolve into components along the b_1 and b_2 directions. The control inputs are given by
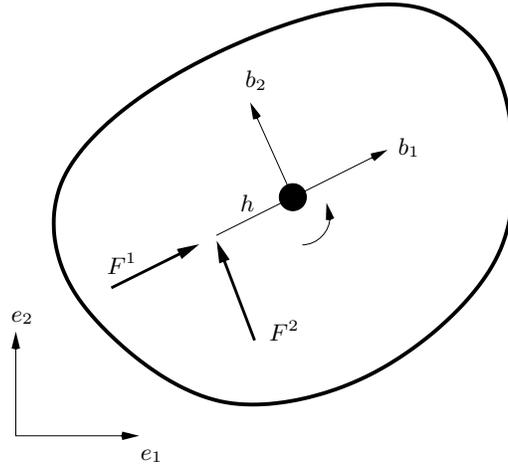
Fig. 2. A schematic of the planar rigid body.

$$F^1 = \cos\theta dx + \sin\theta dy,$$
$$F^2 = -\sin\theta dx + \cos\theta dy - hd\theta.$$

Using Lemma 1, we determine that

$$\frac{ds}{dt} = \frac{\sqrt{2}}{2}w^1(t)w^2(t) - \frac{1}{2}s(t)w^1(t).$$

It also follows from Definition 3 that the symmetric form is given by

$$B_{12} = B_{21} = -\frac{1}{2}\langle\langle\langle Y_1 : Y_2\rangle, Y^\perp\rangle\rangle = \frac{\sqrt{2}}{4}$$

$$B_{11} = B_{22} = 0.$$

Figure 3 is a simulation of the stopping algorithm driving the planar rigid body to rest given the initial velocities $w^1(0) = -10$, $w^2(0) = 5$ and $s(0) = -60$.

4.2 Snakeboard

In this section we review the geometric model of the snakeboard (SB) (Fig. 4).

The configuration manifold for SB is $SE(2) \times \mathbb{S} \times \mathbb{S}$ with local coordinates $(x, y, \theta, \psi, \phi)$. The Riemannian metric is given by

$$\mathbb{G} = mdx \otimes dx + mdy \otimes dy + l^2 md\theta \otimes d\theta$$
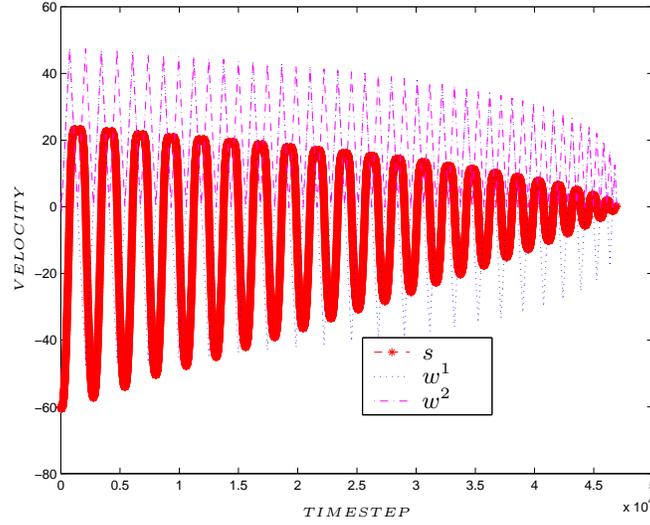$$+ J_r d\psi \otimes d\theta + J_r d\theta \otimes d\psi + J_r d\psi \otimes d\psi + J_w d\phi \otimes d\phi,$$

Fig. 3. A simulation of the stopping algorithm applied to the planar rigid body.
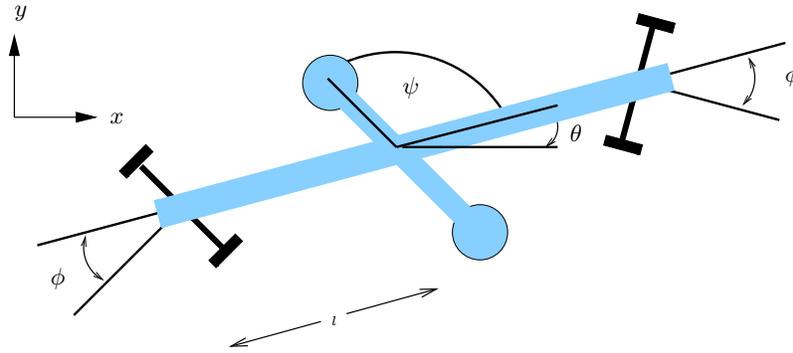

Fig. 4. A schematic of the snakeboard.

where $m > 0$ is the total mass of SB, $J_r > 0$ is the moment of inertia of the rotor mounted on top of the body's center of mass, and $J_w > 0$ is the moment of inertia of the wheel axles. The constraint one-forms are given by

$$0 = \sin(\phi - \theta)\, dx + \cos(\phi - \theta)\, dy + l\cos(\phi)\, d\theta,$$
$$0 = -\sin(\phi + \theta)\, dx + \cos(\phi + \theta)\, dy - l\cos(\phi)\, d\theta.$$

The two control forces are pure torques $F^1 = d\psi$ and $F^2 = d\phi$.

Using Lemma 1, we determine that

$$\frac{ds}{dt} = 2\left\{ -\cos(\phi)\sqrt{\frac{1}{10\cos(2\phi) + 30}} \right\} w^1(t)w^2(t)$$

It also follows from Definition 3 that the symmetric form is given by

$$B_{12} = B_{21} = -\frac{1}{2}\langle\langle\langle Y_1 : Y_2\rangle, Y^\perp\rangle\rangle = -\cos(\phi)\sqrt{\frac{1}{10\cos(2\phi) + 30}}$$

$$B_{11} = B_{22} = 0$$

Figure 5 is a simulation of the stopping algorithm driving the snakeboard to rest given the initial velocities $w^1(0) = 5$, $w^2(0) = -3$ and $s(0) = 10$.
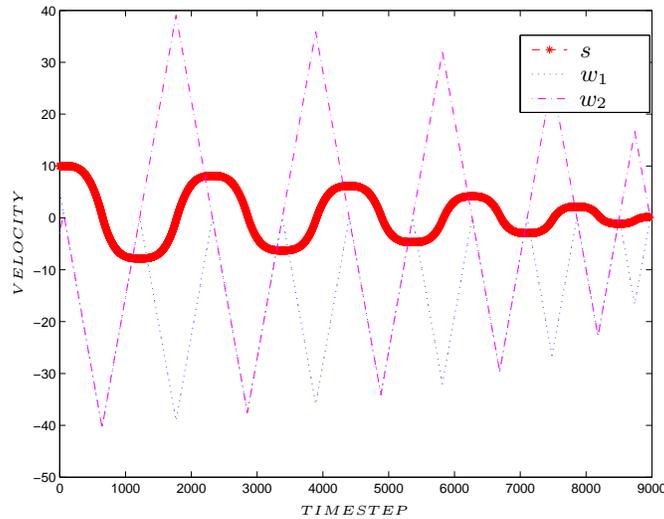

Fig. 5. A simulation of the stopping algorithm applied to the snakeboard.

4.3 Planar Rollerblader

The schematic model and description of the planar rollerblader (RB) can be found in the introduction of this paper. The configuration manifold for RB is $SE(2) \times \mathbb{S} \times \mathbb{R} \times \mathbb{S} \times \mathbb{R}$ with local coordinates $(x, y, \theta, \gamma_1, d_1, \gamma_2, d_2)$. The Riemannian metric is given by

$$\mathbb{G} = \left(m + \frac{M}{2}\right) dx \otimes dx + \frac{1}{2}(d_1 m \cos(\gamma_1) - d_2 m \cos(\gamma_2)) dx \otimes d\theta$$

$$+ \frac{1}{2} d_1 m \cos(\gamma_1) dx \otimes d\gamma_1 + \frac{1}{2} m \sin(\gamma_1) dx \otimes dd_1$$

$$- \frac{1}{2} d_2 m \cos(\gamma_2) dx \otimes d\gamma_2 + \frac{1}{2} m \sin(\gamma_2) dx \otimes dd_2$$

$$+ \left(m + \frac{M}{2}\right) dy \otimes dy + \frac{1}{2}(d_1 m \sin(\gamma_1) - d_2 m \sin(\gamma_2)) dy \otimes d\theta$$

$$+ \frac{1}{2} d_1 m \sin(\gamma_1) dy \otimes d\gamma_1 - \frac{1}{2} m \cos(\gamma_1) dy \otimes dd_1$$

$$- \frac{1}{2} d_2 m \sin(\gamma_2) dy \otimes d\gamma_2 + \frac{1}{2} m \cos(\gamma_2) dy \otimes dd_2$$

$$+ \frac{1}{2}(d_1 m \cos(\gamma_1) - d_2 m \cos(\gamma_2)) d\theta \otimes dx + \frac{1}{2}(d_1 m \sin(\gamma_1) - d_2 m \sin(\gamma_2)) d\theta \otimes dy$$

$$+ \left(mb^2 + d_1 m \cos(\gamma_1) b + d_2 m \cos(\gamma_2) b + \frac{I_c}{2} + I_p + \frac{d_1^2 m}{2} + \frac{d_2^2 m}{2}\right) d\theta \otimes d\theta$$

$$+ \frac{1}{2} \left(m d_1^2 + bm \cos(\gamma_1) d_1 + I_p\right) d\theta \otimes d\gamma_1 + \frac{1}{2} bm \sin(\gamma_1) d\theta \otimes dd_1$$

$$+ \frac{1}{2} \left(m d_2^2 + bm \cos(\gamma_2) d_2 + I_p\right) d\theta \otimes d\gamma_2 + \frac{1}{2} bm \sin(\gamma_2) d\theta \otimes dd_2$$

$$+ \frac{1}{2} d_1 m \cos(\gamma_1) d\gamma_1 \otimes dx + \frac{1}{2} d_1 m \sin(\gamma_1) d\gamma_1 \otimes dy$$

$$+ \frac{1}{2} \left(m d_1^2 + bm \cos(\gamma_1) d_1 + I_p\right) d\gamma_1 \otimes d\theta + \left(\frac{m d_1^2}{2} + \frac{I_p}{2}\right) d\gamma_1 \otimes d\gamma_1$$

$$+ \frac{1}{2} m \sin(\gamma_1) dd_1 \otimes dx - \frac{1}{2} m \cos(\gamma_1) dd_1 \otimes dy$$

$$+ \frac{1}{2} bm \sin(\gamma_1) dd_1 \otimes d\theta + \frac{m}{2} dd_1 \otimes dd_1$$

$$- \frac{1}{2} d_2 m \cos(\gamma_2) d\gamma_2 \otimes dx - \frac{1}{2} d_2 m \sin(\gamma_2) d\gamma_2 \otimes dy$$

$$+ \frac{1}{2} \left(m d_2^2 + bm \cos(\gamma_2) d_2 + I_p\right) d\gamma_2 \otimes d\theta + \left(\frac{m d_2^2}{2} + \frac{I_p}{2}\right) d\gamma_2 \otimes d\gamma_2$$

$$+ \frac{1}{2} m \sin(\gamma_2) dd_2 \otimes dx + \frac{1}{2} m \cos(\gamma_2) dd_2 \otimes dy$$

$$+ \frac{1}{2} bm \sin(\gamma_2) dd_2 \otimes d\theta + \frac{m}{2} dd_2 \otimes dd_2.$$

Let the mass and rotational inertia of the central platform of the robot be M and I_c respectively. Let each link have a rotational inertia I_p. The mass of the link is assumed to be negligible. Each roller blade has mass m, but is assumed to have no rotational inertia. The constraint one-forms are given by

$$0 = -\sin(\theta + \gamma_1) dx + \cos(\theta + \gamma_1) dy - b \sin(\gamma_1) d\theta - dd_1$$
$$0 = -\sin(\theta + \gamma_2) dx + \cos(\theta + \gamma_2) dy - b \sin(\gamma_2) d\theta + dd_2.$$

The four control forces consist of two torques $F^1 = d\gamma_1$ and $F^2 = d\gamma_2$, as well as, two linear actuators $F^3 = dd_1$ and $F^4 = dd^2$.

Here we only include the simulation results due to the complexity associated with the symbolic representation of the symmetric form. Figure 6 is a simulation of the stopping algorithm driving the planar rollerblader to rest given the initial velocities $w^1(0) = 1$, $w^2(0) = -1$, $w^3(0) = 2$, $w^4(0) = -5$ and $s(0) = 10$.
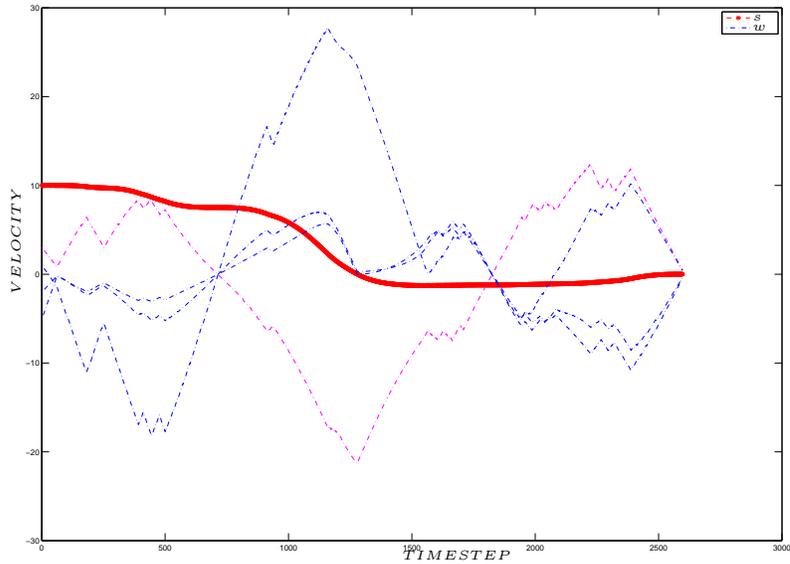

Fig. 6. A simulation of the stopping algorithm applied to the planar rollerblader.

5 Conclusions

We seek to extend our results to mechanical systems underactuated by an arbitrary number of controls. This will involve characterizing coordinate invariant properties of the intrinsic *vector-valued* symmetric bilinear form that allow motion in the input foliation.

References

1. F. Bullo and A. Lewis. *Geometric Control of Mechanical Systems.* Springer Science+Business Media, New York, NY, 2005.

2. F. Bullo and A. Lewis. *Low-order controllablility and kinematic reductions for affine connection control systems.* SIAM Journal on Control and Optimization 44(3):885-908, 2005.
3. F. Bullo and A. Lewis. *Kinematic controllability and motion planning for the snakeboard.* IEEE Transactions on Robotics and Automation 19(3):494-498, 2003.
4. J.P. Ostrowski, J.P. Desai and V. Kumar. *Optimal gait selection for nonholonomic locomotion systems.* The International Journal of Robotics Research 19(5):225-237, 2000.
5. F. Bullo and M. Zefran. *On mechanical control systems with nonholonomic constraints and symmetries*, Systems and Control Letters 45(2):133-143, 2002.
6. R. Hirschorn and A. Lewis. *Geometric local controllability: second-order conditions.* Proceedings of the 41st IEEE CDC, 1:368-369, December 2002.
7. F. Bullo, J. Cortes, A. Lewis, and S. Martinez *Vector-valued quadratic forms in control theory* Sixty Open Problems in Mathematical Systems and Control Theory, V. Blondel and A. Megretski (Eds.), Princeton University Press, 315-320, 2004.
8. S. Chitta and V.J. Kumar. *Dynamics and generation of gaits for a planar rollerblader.* Proceedings of the 2003 IEEE IROS, 1:860-865, 2003.
9. A. Lewis, J.P. Ostrowski, R. Murray and J. Burdick. *Nonholonomic mechanics and locomotion: the snakeboard example.* Proceedings of the 1994 IEEE ICRA, 2391-2400, 1994.
10. F. Bullo and R. Murray. *Tracking for fully actuated mechanical systems: A geometric framework.* Automatica. The Journal of IFAC, 35(1):17-34, 1999.
11. A. Lewis. *Simple mechanical control systems with constraints.* IEEE Transactions on Automatic Control, 45(8):1420-1436, August 2000.
12. M.P. do Carmo. *Riemannian Geometry.* Birkhauser, Boston, MA, English edition, 1992.
13. J. Nightingale, R. Hind, B. Goodwine. *Geometric analysis of a class of constrained mechanical control systems in the nonzero velocity setting.* Proceedings of the 2008 IFAC, 2008.
14. J. Nightingale, R. Hind, B. Goodwine. *Intrinsic Vector-Valued Symmetric Form for Simple Mechanical Control Systems in the nonzero velocity setting.* Proceedings of the 2008 IEEE ICRA, 2008.